

# Preparation and Thermal Properties of Hexadecanol-Myristic Acid Eutectics/Activated Carbon Composites as Shape-stabilized Phase Change Materials in Thermal Energy Storage

Yanghua CHEN \*, Zhaohe WANG, Minrong GE, Feng ZHAO

College of Mechatronics Engineering, Nanchang University, Nanchang 330031, China

**crossref** <http://dx.doi.org/10.5755/j02.ms.24883>

Received 17 December 2019; accepted 29 April 2020

In this study, hexadecanol-myristic acid (HD-MA) binary eutectic mixtures were adsorbed into activated carbon (AC) to prepare the composite phase transition materials (CPCMs). In the hexadecanol-myristic acid/activated carbon (HD-MA/AC) composites, the mixture of HD-MA acted as the phase change energy storage material and the AC was used as the matrix supporting material. Activated carbon is a kind of inorganic supporting material, which has developed pore structure, strong adsorption, high mechanical strength, corrosion resistance and good thermal stability. As the supporting material, activated carbon was helpful to prevent the eutectics from leakage. The chemical structure and crystal phase structure of HD-MA/AC composites were tested by FT-IR and XRD. The microstructure of the composites was observed through field emission scanning electron microscopy (FE-SEM). It was found that the organic binary eutectics were adsorbed on the surface and inside by activated carbon. Thermal properties of the composites were measured by differential scanning calorimetry (DSC). The results of performance test demonstrated that the satisfactory sample CPCM1 melted at 42.38 °C with latent heat of 76.24 J/g and solidified at 38.32 °C with latent heat of 67.08 J/g. The test results of TGA indicated that the prepared composites of hexadecanol-myristic acid/activated carbon possessed great thermal stability and high reliability. It is predicted that the shape-stabilized HD-MA/AC composites have great potential for thermal energy storage.

**Keywords:** composite phase change materials, eutectics, activated carbon, shape-stabilized, thermal properties.

## 1. INTRODUCTION

In recent years, owing to the rapidly increase in global energy consumption and the lack of fossil fuel resources, people have increasingly paid attention to energy storage issues. Thermal energy storage usually includes various forms such as latent heat storage, sensible heat storage and thermochemical energy storage. In particular, latent heat storage primarily based on the use of phase change material is considered the prime method to obtain higher thermal performance. Latent heat storage, also known as phase transition energy storage, is achieved by absorbing and releasing thermal energy in the course of phase transition. Latent heat storage is significantly better than sensible heat storage in terms of energy storage density, appropriate phase transition temperature and contribution to environment friendly during energy utilization [1, 2]. Due to the phase change materials absorb and release energy in a small range even at almost constant temperature pending the phase change transition, they are considered as ideal thermal energy storage materials [3, 4]. So far, people have studied series of phase transition energy storage materials including brine, alkanes, fatty acids and fatty alcohols. They have been widely used in many spheres, such as building systems [5, 6], air conditioning [7–9], textiles [10], solar energy storage [11] and thermal management of electronic equipment [12], etc.

Organic fatty acids and fatty alcohols have the advantages of large latent heat, small volume change, no

transition separation, low subcooling, non-toxicity, good thermal reliability and low price. Thus, they are widely applied in thermal energy storage [13–17]. However, some disadvantages have largely limited the application of fatty acids and fatty alcohols, such as leakage of liquid phase change materials during melting. In order to prevent fatty acids and fatty alcohols from leakage, by using microcapsule technology and porous matrix material supporting technology, the composite phase change materials still maintain stable form in the course of phase transition. Because the phase transition energy storage materials are wrapped by the matrix supporting materials, only the internal phase change materials undergo change when the phase transition occurs. And the supporting materials do not undergo phase transition process, thus they prevent the internal materials from leaking [18–24]. A plenty of materials have been exploited as matrix supporting materials, for example, activated carbon, expanded graphite, expanded perlite, diatomite, and polyurethane rigid foam, etc. [25–29].

Previous studies have involved thermal properties of organic fatty acids and have made performance comparisons with different supporting materials in some literatures. However, the CPCMs of organic fatty acids and alcohol binary eutectics are rarely involved and few literatures have investigated their thermal properties. Sari et al. [30, 31] studied some fatty acids, prepared a series of eutectics mixtures and measured the thermal reliability. Cao et al. [32] prepared the lauric acid-stearic acid eutectics/cellulose CPCMs by using a porous matrix adsorption method and the

\* Corresponding author. Tel.: +86-13970944938.  
E-mail address: [chyhix@163.com](mailto:chyhix@163.com) (Y. Chen)

outcomes declared that fatty acid eutectics adsorbed well in polyporate structure of cellulose. Tang et al. [33] adsorbed palmitic acid-decanoic acid cocrystal into diatomite. When mass ratio of the eutectic mixtures and diatomite was 2:1, the sample melts at 26.69 °C with latent heat of 98.26 kJ/kg and solidifies at 21.85 °C with latent heat of 90.03 kJ/kg, which can be used as a kind of shape-stabilized CPCMs for heat energy storage.

So far, the preparation and thermal properties of hexadecanol-myristic acid/activated carbon CPCMs have not been reported. This article researched the preparation and thermal properties of hexadecanol-myristic acid/activated carbon shape-stabilized CPCMs. In the composites, the HD-MA eutectics acted as phase transition storage materials and the activated carbon was used as the matrix supporting material. Activated carbon had such properties owing to its small diameters and large surface areas. Thus, it was an excellent inorganic porous material, which can better encapsulate phase change energy storage materials. HD-MA/AC shape-stabilized composite phase transition materials will have a broad application in solar heating and building energy saving systems due to the suitable phase transition temperature and high enthalpy.

## 2. EXPERIMENT

### 2.1. Materials

The phase transition temperatures of hexadecanol (C<sub>16</sub>H<sub>34</sub>O, AR) and myristic acid (C<sub>14</sub>H<sub>28</sub>O<sub>2</sub>, AR) were 47.6 °C and 54.8 °C, respectively. Their phase transition enthalpies were 240.8 J/g and 189 J/g, respectively. Activated carbon (≥ 200 mesh) was chosen as the matrix supporting material. The three materials above were all from Aladdin Chemical Reagent Co., Ltd.

### 2.2. Preparation of the HD-MA eutectics

Schroder's formula is a very important formula based on the phase equilibrium theory and the second law of thermodynamics. Given the phase transition temperature and latent heat of the binary eutectics component, the relationship between the eutectics point of the binary mixture and the molar fraction of the corresponding component *i* can be predicted theoretically.

The Schrader equation is presented as follows [34]:

$$T = \left( \frac{1}{T_i} - \frac{R \ln x_i}{\Delta H_i} \right)^{-1} \quad i=A,B, \quad (1)$$

where  $T_i$ ,  $\Delta H_i$  and  $x_i$  represent the phase change temperature, the latent heat of phase transition and the mole fraction of component, respectively.  $T$  indicates the phase change temperature of the mixtures.  $R$  represents the gas constant (8.314 J/(K·mol)).  $x_A$  and  $x_B$  are the mole fractions of components A and B in the binary eutectics ( $x_A + x_B = 1$ ).

The latent heat of phase transition of the binary eutectics is from the following formula [34]:

$$H = T \sum_{i=1}^n \left[ \frac{x_i H_i}{T_i} \right] + T \sum_{i=1}^n \left[ x_i (C_{PLi} - C_{PSi}) \ln \left( \frac{T}{T_i} \right) \right]$$

$$(i = A, B), \quad (2)$$

where  $H$  is the latent heat of the eutectics phase transition, J/mol;  $C_{PSi}$  and  $C_{PLi}$  are the constant pressure specific heat capacities of component  $i$  in the solid and liquid states, respectively.

$T \sum_{i=1}^n [x_i (C_{PLi} - C_{PSi}) \ln(T/T_i)]$  indicates the sensible heat of the mixtures, which is negligible due to its small value. So the formula is simplified as flowing:

$$H = T \sum_{i=1}^n \left( \frac{x_i H_i}{T_i} \right) \quad (i = A, B). \quad (3)$$

According to Eq. 1 the predicted phase diagram of the binary eutectics of hexadecanol and myristic acid is shown in Fig. 1. It could be seen that the molar fraction of the hexadecanol component corresponding to the eutectics point was 58 %. A kind of mixture of hexadecanol and myristic acid in a molar fraction ratio of 58 : 42 (that is mass ratio of hexadecanol: myristic acid = 59.4 : 40.6) was used as the eutectic phase transition materials. Meanwhile, the latent heat of the hexadecanol and the myristic acid mixture corresponding to the eutectics point was calculated by Eq. 3. The theoretical value was 37698 J/mol, which was 159.63 J/g.

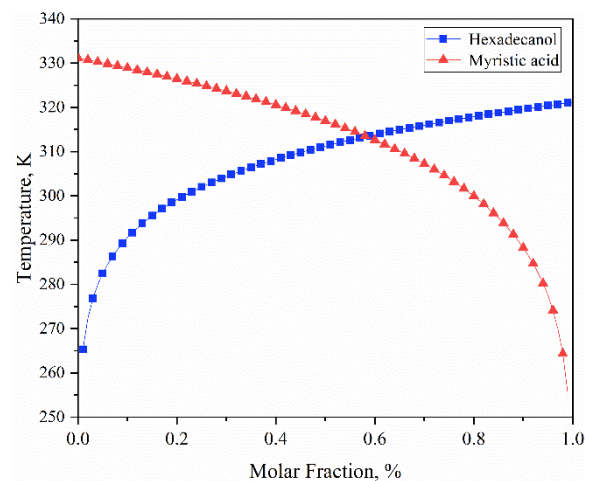


Fig. 1. The predicted phase diagram of the hexadecanol-myristic acid binary eutectics

### 2.3. Preparation of the HD-MA/AC composites

Firstly, a certain amount of activated carbon was weighed and put in a beaker, and dried in a vacuum drying oven at 80 °C for 24 hours to release the gas which existed in the pores of the activated carbon. Mixed the hexadecanol-myristic acid (mass ratio HD:MA = 59.4 : 40.6) mixture in a beaker uniformly, then put the beaker in a thermostatic magnetic stirring water bath to maintain a water temperature of 70 °C and kept the stirring speed at 500 rpm/min for 1 h until the mixture materials melting well and completely. Next, dried activated carbon was added to the beaker and thermostatic magnetic stirring water bath still maintained the original temperature and the stirring speed until the activated carbon adsorbed the binary eutectics completely. The mixture got cooled close to room temperature, then it

was placed in a vacuum drying box and dried at 35 °C for 24 h to remove moisture therefrom. Ultimately, five HD-MA/AC composite phase transition material samples were prepared, which were recorded as CPCM1, CPCM2, CPCM3, CPCM4 and CPCM5, respectively. Their composition is given in Table 1.

**Table 1.** The composition of HD-MA eutectics and AC

Samples	HD, g	MA, g	AC, g
CPCM1	5.94	4.06	6.7
CPCM2	5.94	4.06	8.2
CPCM3	5.94	4.06	10
CPCM4	5.94	4.06	12.2
CPCM5	5.94	4.06	15

## 2.4. Characterization of the HD-MA/AC composites

The morphology of activated carbon and five samples were observed by field emission scanning electron microscopy (FE-SEM, JSM6701F, JEOL, Japan). The chemical structures of five samples, activated carbon and HD-MA eutectics were analyzed by FT-IR (Nicolet5700). The infrared spectra with a frequency of 4000  $\text{cm}^{-1}$  to 400  $\text{cm}^{-1}$  were recorded by KBr method with an accuracy of 0.09  $\text{cm}^{-1}$ . Differential scanning calorimeter (DSC, DSC8000) was employed to measure thermal properties of the samples. The heating and cooling rate were both 5 °C/min and the measurement process was under in nitrogen environment of 20 ml/min. The thermogravimetric analyzer (TGA4000, PE) was employed to measure thermal stability of the eutectics, activated carbon and five samples. In addition, the program controlled the temperature to rise from room temperature to 700 °C at the rate of 20 °C/min. The measurement process was under in nitrogen protection.

## 3. RESULTS AND DISCUSSION

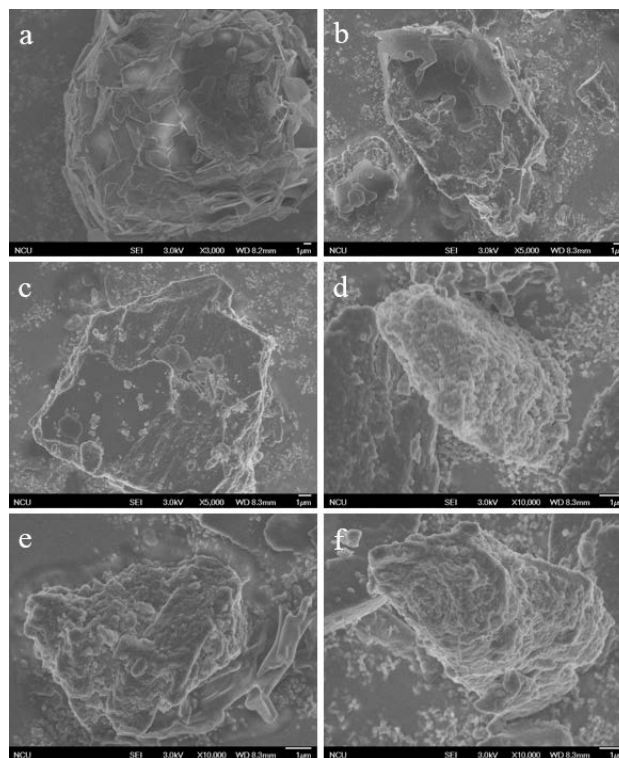
### 3.1. SEM analysis

Fig. 2. shows the micro morphology of activated carbon and CPCM1-CPCM5. Fig. 2 a shows the micro-morphology of activated carbon. It can be seen that the surface of activated carbon was rough, the pore structure was well-developed and the internal specific surface area was large. It can be filled to a saturated state by the molten eutectic mixtures. As shown in Fig. 2 b to f, through the capillary force and surface tension between the eutectics and activated carbon, binary eutectics (CPCM1 (60 wt.%), CPCM2 (55 wt.%), CPCM3 (50 wt.%), CPCM4 (45 wt.%), CPCM5 (40 wt.%)) were well adsorbed into the pore structure of activated carbon. Stimulated by high-energy electron beams, composite phase transition materials still had relatively regular shape structure. It indicated that the activated carbon could provide certain mechanical strength for molten eutectics and prevent molten eutectics from leakage. This result was consistent with other literatures which used carbon family as supporting material [15, 25].

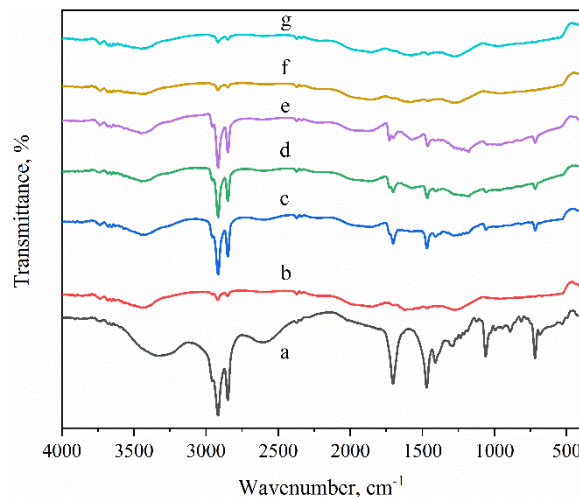
### 3.2. FT-IR analysis

Fig. 3. displays the FT-IR spectra of HD-MA eutectics, activated carbon and CPCM-CPCM5. The spectrum of HD-MA eutectics is presented in Fig. 3 a. The absorption peaks

at 3328  $\text{cm}^{-1}$  and 2605  $\text{cm}^{-1}$  correspond to the stretching vibration and bending vibration of -OH group in water molecules.



**Fig. 2.** SEM images of the activated carbon and CPCM1-CPCM5: a–activated carbon (3 k $\times$ ); b–CPCM1 (5 k $\times$ ); c–CPCM2 (5k $\times$ ); d–CPCM3 (10k $\times$ ); e–CPCM4 (10 k $\times$ ); f–CPCM5 (10k $\times$ )



**Fig. 3.** FT-IR spectra: a–HD-MA eutectics; b–activated carbon; c–CPCM1; d–CPCM2; e–CPCM3; f–CPCM4; g–CPCM5

The characteristic peaks of 2917  $\text{cm}^{-1}$  and 2848  $\text{cm}^{-1}$  indicated the antisymmetric and symmetric stretching vibrations of their -CH<sub>2</sub> groups. The absorption peaks at 1706  $\text{cm}^{-1}$  and 1471  $\text{cm}^{-1}$  indicated the in-plane bending vibration of -OH functional groups. A series of characteristic peaks from 1411.64  $\text{cm}^{-1}$  to 970  $\text{cm}^{-1}$  demonstrated the bending vibration of -OH group in the plane. The absorption peaks at 1060  $\text{cm}^{-1}$  and 717  $\text{cm}^{-1}$  revealed the out of plane bending vibration of -OH group

and C–H bond, respectively. From  $1006\text{ cm}^{-1}$  to  $696\text{ cm}^{-1}$ , the absorption peak represented the in-plane swing vibration peak of –OH functional group in eutectics. The spectrum of the activated carbon is shown in Fig. 3 b. The absorption peaks of  $3774\text{ cm}^{-1}$ ,  $3149\text{ cm}^{-1}$  and  $1099\text{ cm}^{-1}$  were caused by the vibration of –OH group in the water molecules absorbed by the activated carbon [25]. The peak at  $1297\text{ cm}^{-1}$  demonstrated the bending vibration of –CH<sub>3</sub> group C–H bond in the plane.

Fig. 3 c to g respectively represent the spectra of CPCM1 to CPCM5. From Fig. 3 c to g, it can be seen that the spectrum from CPCM1 to CPCM5 covered all the characteristic absorption peaks of eutectics and active carbon, indicating that there was only physical adsorption between the eutectics and active carbon without chemical reaction, new peak and displacement of the original absorption peak. This illustrated that the eutectics were adsorbed into activated carbon well.

### 3.3. XRD analysis

Fig. 4. displays the XRD patterns of HD-MA eutectics, activated carbon and CPCM1-CPCM5. Fig. 4 a displays the XRD pattern of myristic acid. The peaks of  $16.9^\circ$ ,  $18.3^\circ$ ,  $21.9^\circ$ ,  $23.6^\circ$ ,  $28.1^\circ$ , and  $34.1^\circ$  were due to the regular crystallization of HD-MA eutectics. Fig. 4 b displays an XRD pattern of activated carbon.

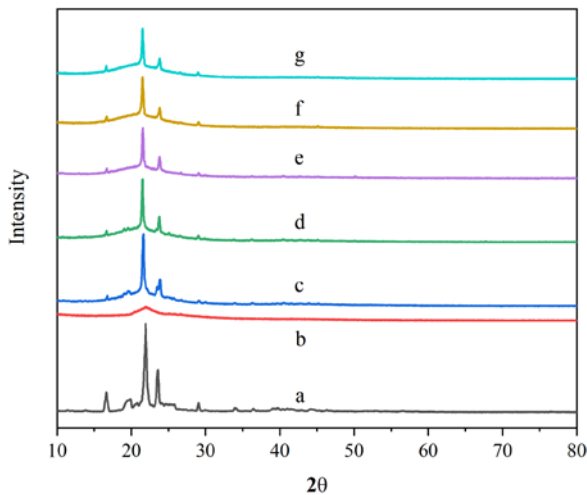


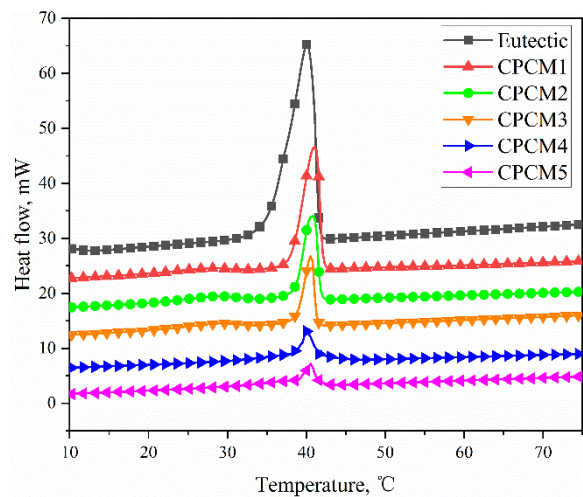
**Fig. 4.** XRD patterns: a–HD-MA eutectics; b–activated carbon; c–CPCM1; d–CPCM2; e–CPCM3; f–CPCM4; g–CPCM5

It can be seen that there was a flat peak around  $23.5^\circ$ , which illustrated that the activated carbon was porous structure. It can be known from Fig. 4 c to g that the XRD peaks of HD-MA eutectics also appeared in the XRD patterns of CPCM and the flat peaks of activated carbon also appeared in the composite patterns. Because CPCM contained activated carbon, their peak heights were much lower than that of HD-MA eutectic and its crystallinity was not as good as that of eutectic mixtures. The results indicated that the crystal structure of the HD-MA eutectics in the composite phase transition materials remained unchanged.

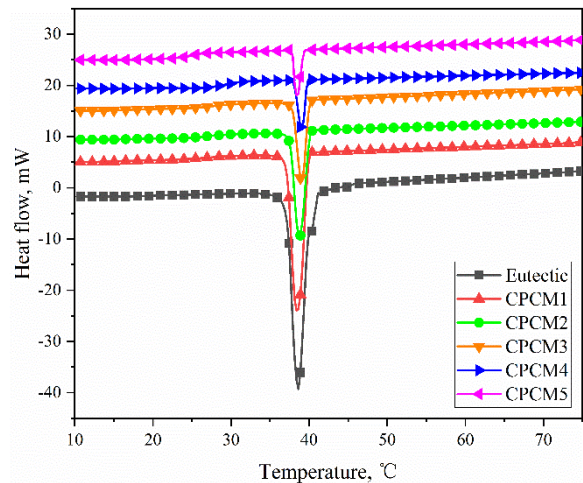
### 3.4. Thermal properties analysis

Fig. 5 and Fig 6 are the DSC curves of the melting and solidification processes of HD-MA eutectics and CPCM1-

CPCM5, respectively. Table 2. displays the thermal performance parameters. As can be seen from the graphs, the HD-MA eutectic melted at  $40.77^\circ\text{C}$  and solidified at  $39.34^\circ\text{C}$ . The melting and solidifying latent heats were determined to be  $158.49\text{ J/g}$  and  $147.12\text{ J/g}$ , respectively. For CPCM1, it melted at  $42.38^\circ\text{C}$  and solidified at  $38.32^\circ\text{C}$ . The melting and solidifying latent heat values were determined to be  $76.24\text{ J/g}$  and  $67.08\text{ J/g}$ . In Fig. 5 and Fig. 6, the melting and solidification peaks of the DSC curves showed the similar endothermic and exothermic peaks. The results manifested that the mixture of hexadecanol and myristic acid in the prepared materials formed a good eutectics system. The melting and solidification processes signified that the experimental results were consistent with theoretical prediction.



**Fig. 5.** The melting DSC curves of the HD-MA eutectics, CPCM1, CPCM2, CPCM3, CPCM4, CPCM5



**Fig. 6.** The solidifying DSC curves of the HD-MA eutectics, CPCM1, CPCM2, CPCM3, CPCM4, CPCM5

It can be known from Table 2 that the phase change latent heat values of five samples were lower than pure HD-MA eutectics in the materials. Because during the phase transition, only the HD-MA eutectics could absorb/release heat and the activated carbon had no thermal effect. So, the phase transition latent heat values of CPCM was lower than that of pure HD-MA eutectics system. Moreover, the latent heat value of CPCM reduced as the mass fraction of HD-MA eutectics in CPCM decreased.

**Table 2.** DSC values of the HD-MA eutectics and CPCM1-CPCM5

Samples	Melting process			Solidification process			Mass fraction of HD-MA eutectics, %
	$T_{onset}$ , °C	$T_{peak}$ , °C	Latent heat, J/g	$T_{onset}$ , °C	$T_{peak}$ , °C	Latent heat, J/g	
HD-MA	37.57	40.77	158.49	44.79	39.34	147.12	100
CPCM1	38.65	42.38	76.24	42.06	38.32	67.08	60
CPCM2	38.36	42.19	63.58	41.82	38.29	57.24	55
CPCM3	38.23	41.90	44.21	41.45	38.54	36.16	50
CPCM4	38.21	41.25	36.91	41.09	38.26	25.07	45
CPCM5	38.15	40.32	23.86	40.55	37.84	20.12	40

**Table 3.** Comparison of thermal properties of phase change materials in this article and other literatures

Materials	Type	Melting point, °C	Melting enthalpy, J/g	Solidifying point, °C	Solidifying enthalpy, J/g	Application	References
MA-LA/EG	composite	34.29	122.8	32.94	115.4	Thermal energy storage	[35]
TD-MA/CMC	composite	34.61	102.11	31.09	84.58	Thermal energy storage	[36]
MA-SA/CNTs	composite	45.51	166.49	41.10	168.79	Thermal energy storage	[37]
HD-SA/BC	composite	45.29	68.85	43.68	61.41	Thermal energy storage	[38]
HD-MA/AC	composite	42.38	76.24	38.32	67.08	Thermal energy storage	Present study

Table 3 demonstrated the contrast of thermal performance parameters of the CPCMs, which has been made in this experiment with other literature composite phase transition materials. It is cleared that the satisfactory HD-MA/AC composite phase change material had suitable phase transition temperature and large latent heat value. In addition, activated carbon could be used as a nucleating agent during the solidification of eutectics, aiming at reducing the degree of subcooling and enabling the composite phase change materials to respond to temperature changes in time. Day and night temperature fluctuations made people in room more comfortable.

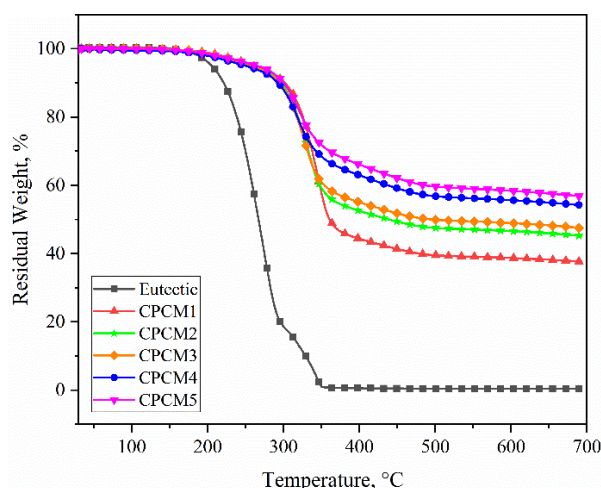
### 3.5. Thermal stability analysis

Fig. 7 is TGA curves of HD-MA binary eutectics and CPCM1-CPCM5. The initial temperature ( $T_{onset}$ ) at the mass loss, the corresponding temperature ( $T_{peak}$ ) at the maximum mass loss rate and the residual quantity at 700 °C of the HD-MA eutectics and the five samples were recorded in Table 4.

**Table 4.** TGA values of HD-MA eutectics and CPCM1-CPCM5

Samples	$T_{onset}$ , °C	$T_{peak}$ , °C	Percentage of the residual mass, % (700 °C)
HD-MA eutectics	181.76	242.56	0 (346 °C)
CPCM1	198.63	337.89	37.63
CPCM2	206.51	339.26	45.18
CPCM3	203.43	343.37	47.50
CPCM4	204.46	348.51	54.18
CPCM5	207.20	357.06	56.77

From Fig. 7, we can see that HD-MA eutectics had only one thermal decomposition process. The thermal decomposition curve trends of CPCM1-CPCM5 were basically the same and relatively mild, indicating that the thermal decomposition rate of the prepared composites was lower than that of eutectic materials.

**Fig. 7.** The TGA analysis of HD-MA eutectics and CPCM1-CPCM5

In Table 5, it can be cleared that the remaining amount of HD-MA eutectics at 346 °C was almost zero and the residual amounts of CPCM1, CPCM2, CPCM3, CPCM4, and CPCM5 at this degree temperature were 57.62 %, 59.15 %, 60.92 %, 68.43 %, 71.81 %. The TGA analysis results were basically consistent with the DSC analysis results. As the mass fraction of activated carbon increased in the composite phase transition materials, the residual amount of the samples increased too. The above results demonstrated that activated carbon which acted as a supporting material prevented the liquid phase transition material from leakage by establishing a carbon layer as a physical protective barrier. It was declared that the prepared composite materials possessed good thermal stability.

### 3.6. Thermal cycle analysis

The change of sample mass after 1200 cycles of melting and solidification was shown in Table 5. It can be seen from Table 5 that after the first 100 thermal cycles, the mass loss

rate of the sample was 0.36 %, and the mass loss rate reached 1.07 % after 1200 cycles. After 200 thermal cycles, the mass of the composite phase change material hardly changed. There were no oil stains appeared on the filter paper during the thermal cycling experiment of the composite phase change material, indicating that there is no leakage of the phase change material, which proves that the composite phase change material has good adsorption effect and good heat stability. It can be used in many fields such as building energy storage and solar energy storage systems.

**Table 5.** The mass change of HD-MA/AC composite phase change materials after thermal cycling

Thermal cycles	Mass, g	Mass loss rate, %
1	0.5406	0
100	0.5387	0.36
200	0.5335	0.97
400	0.5280	1.03
600	0.5226	1.03
800	0.5172	1.04
1000	0.5117	1.07
1200	0.5062	1.07

#### 4. CONCLUSIONS

In this work, the preparation and thermal properties of the HD-MA/AC composite phase change materials were discussed. The HD-MA eutectics acted as the energy storage materials and the AC was used as the matrix supporting material. Because of the effects of capillary force and surface tension, the HD-MA eutectics were soaked up by the strong adsorptive AC, which was showing the uniform distribution in the CPCMs without chemical action. In this study, the satisfactory shape-stabilized HD-MA/AC sample CPCM1 melted at 42.38 °C and solidified at 38.32 °C. The melting and solidifying latent heat values were determined to be 76.24 J/g and 67.08 J/g. Compared with other samples, CPCM1 has better phase transition temperature, higher latent heat and better thermal stability. In addition, TGA research indicated that the CPCMs possessed great thermal stability and high reliability. In summary, the shape-stabilized HD-MA/AC composites possess the characteristics of stable shape, suitable phase change temperature, high phase transition enthalpy, great thermal stability and high reliability. It is concluded that the prepared shape-stabilized composite phase transition materials will develop a brilliant application prospect in the realm of energy storage and building construction.

#### Acknowledgments

This work was supported by the Science and Technology Supporting Program of Jiangxi Province, China (No. 20112BBE50031). The authors also wish to thank the reviewers and editor for kindly giving revising suggestions.

#### REFERENCES

1. Wu, J., Long, X.F. Research Progress of Solar Thermochemical Energy Storage *Chemical Progress* 33 (12) 2014: pp. 3238–3244. <https://doi.org/10.1002/er.3259>
2. Yuan, Y.P., Xiang, B., Cao, X.L., Zhang, N., Sun, L.L. Research Status and Development on Latent Energy Storage Technology of Building *Journal of Southwest Jiaotong University* 51 (3) 2016: pp. 3238–3244. <https://doi.org/10.3969/j.issn.0258-2724.2016.03.017>
3. Zhang, Z., Shi, G., Wang, S., Fang, X., Liu, X. Thermal Energy Storage Cementmortar Containing Noctadecane/Expanded Graphite Composite Phase Change Material *Renewable Energy* 50 2013: pp. 670–675. <https://doi.org/10.1016/j.renene.2012.08.024>
4. Zeng, J.L., Zeng, S.H., Zheng, S.B., Yu, F.R., Zhu, J., Gan, L., Zhu, Z.L., Xiao, X.Y., Zhu, Z., Zhu, L.X., Sun, Z. Myristic Acid/Polyaniline Composites as Form Stable Phase Change Materials for Thermal Energy Storage *Solar Energy Materials & Solar Cells* 114 2013: pp. 136–140. <https://doi.org/10.1016/j.solmat.2013.03.006>
5. Zhou, D., Zhao, C.Y., Tian, Y. Review on Thermal Energy Storage with Phase Change Materials (PCMs) in Building Applications *Applied Energy* 92 2012: pp. 593–605. <https://doi.org/10.1016/j.apenergy.2011.08.025>
6. Konuklu, Y., Ostry, M., Paksoy, H.O., Charvat, P. Review on Using Microencapsulated Phase Change Materials (PCM) in Building Applications *Energy and Buildings* 106 2015: pp.134–155. <https://doi.org/10.1016/j.enbuild.2015.07.019>
7. Navidbakhsh, M., Shirazi, A., Sanaye, S. Four Analysis and Multi-objective Optimization of An Ice Storage System Incorporating PCM as the Partial Cold Storage for Air-conditioning Applications *Applied Thermal Engineering* 58 2013: pp. 30–41. <https://doi.org/10.1016/j.applthermaleng.2013.04.002>
8. Parameshwaran, R., Kalaiselvam, S. Energy Conservative Air Conditioning System Using Silver Nano-based PCM Thermal Storage for Modern Buildings *Energy and Buildings* 69 2014: pp. 202–212. <https://doi.org/10.1016/j.enbuild.2013.09.052>
9. Sanaye, S., Shirazi, A. Thermo-economic Optimization of An Ice Thermal Energy Storage System for Air-conditioning Applications *Energy and Buildings* 60 2013: pp. 100–109. <https://doi.org/10.1016/j.enbuild.2012.12.040>
10. Karaipekli, A., Sari, A. Preparation Thermal Properties and Thermal Reliability of Eutectics Mixtures of Fatty acids/Expanded Vermiculite as Novel Form-stable Composites for Energy Storage *Journal of Industrial & Engineering Chemistry* 16 2010: pp. 767–773. <https://doi.org/10.1016/j.jiec.2010.07.003>
11. Fazilati, M.A., Alemrajabi, A.A. Phase Change Material for Enhancing Solar Water Heater, An Experimental Approach *Energy Conversion & Management* 71 2013: pp. 138–145. <https://doi.org/10.1016/j.enconman.2013.03.034>
12. Kalbasi, R., Salimpou, M.R. Constructural Design of Phase Change Material Enclosures Used for Cooling Electronic Devices *Applied Thermal Engineering* 84 2015: pp. 339–349. <https://doi.org/10.1016/j.applthermaleng.2015.03.031>
13. Li, W., Song, G., Li, S., Yao, Y.W., Tang, G.Y. Preparation and Characterization of Novel MicroPCMs (microencapsulated phase-change materials) with Hybrid Shells Via the Polymerization of Two Alkoxy Silanes *Energy* 70 2014: pp. 298–306. <https://doi.org/10.1016/j.energy.2014.03.125>
14. Yuan, Y.P., Zhang, N., Tao, W.Q., Cao, X.L., He, Y.L. Fatty Acids as Phase Change Materials: A Review *Renewable & Sustainable Energy Reviews* 29 2014: pp. 482–498. <https://doi.org/10.1016/j.rser.2013.08.107>

15. **Sari, A., Karaipekli, A.** Preparation, Thermal Properties and Thermal Reliability of Palmitic Acid/Expanded Graphite Composite as Form-stable PCM for Thermal Energy Storage *Solar Energy Materials & Solar Cells* 93 2009: pp. 571–576.  
<https://doi.org/10.1016/j.solmat.2008.11.057>
16. **Yang, X.J., Yuan, Y.P., Zhang, N., Cao, X.L., Liu, C.** Preparation and Properties of Myristic-palmitic-stearic Acid/Expanded Graphite Composites as Phase Change Materials for Energy Storage *Solar Energy* 99 2014: pp. 259–266.  
<https://doi.org/10.1016/j.solener.2013.11.021>
17. **Li, B.X., Liu, T.X., Hu, L.Y., Wang, Y.F., Nie, S.B.** Facile Preparation and Adjustable Thermal Property of Stearic Acid Egraphene Oxide Composite as Shape-stabilized Phase Change Material *Chemical Engineering Journal* 215 2013: pp. 819–826.  
<https://doi.org/10.1016/j.cej.2012.11.077>
18. **Fang, G.Y., Tang, F., Cao, L.** Preparation Thermal Properties and Applications of Shape-stabilized Thermal Energy Storage Materials *Renewable & Sustainable Energy Reviews* 40 2014: pp. 237–259.  
<https://doi.org/10.1016/j.rser.2014.07.179>
19. **Li, M., Wu, Z.S., Kao, H.T.** Study on Preparation and Thermal Properties of Binary Fatty Acid/Diatomite Shape-stabilized Phase Change Materials *Solar Energy Materials & Solar Cells* 95 2011: pp. 2412–2416.  
<https://doi.org/10.1016/j.solmat.2011.04.017>
20. **Aydin, A.A., Okutan, H.** Polyurethane Rigid Foam Composites Incorporated with Fatty Acid Ester-based Phase Change Material *Energy Conversion & Management* 68 2013: pp. 74–81.  
<https://doi.org/10.1016/j.enconman.2012.12.015>
21. **Sari, A., Karaipekli, A.** Preparation Thermal Properties and Thermal Reliability of Capric Acid/Expanded Perlite Composite for Thermal Energy Storage *Materials Chemistry & Physics* 109 2008: pp. 459–464.  
<https://doi.org/10.1016/j.matchemphys.2007.12.016>
22. **Xu, B.W., Li, Z.J.** Paraffin/Diatomite Composite Phase Change Material Incorporated Cement-based Composite for Thermal Energy Storage *Applied Energy* 105 2013: pp. 229–237.  
<https://doi.org/10.1016/j.apenergy.2013.01.005>
23. **Memon, S.A., Lo, T.Y., Cui, H.Z., Barbhuiya, S.** Preparation, Characterization and Thermal Properties of Dodecanol/Cement as Novel Form-stable Composite Phase Change Material *Energy and Buildings* 66 2013: pp. 697–705.  
<https://doi.org/10.1016/j.enbuild.2013.07.083>
24. **Karaipekli, A., Sari, A.** Capric-myristic Acid/Vermiculite Composite as Form-stable Phase Change Material for Thermal Energy Storage *Solar Energy* 83 2009: pp. 323–332.  
<https://doi.org/10.1016/j.solener.2008.08.012>
25. **Chen, Z., Shan, F., Cao, L., Fang, G.Y.** Preparation and Thermal Properties of Shape-stabilized Lauric Acid/Activated Carbon Composites as Phase Change Materials for Thermal Energy Storage *Solar Energy Materials & Solar Cells* 102 2012: pp. 131–136.  
<https://doi.org/10.1016/j.solmat.2012.03.013>
26. **Karaipekli, A., Sari, A.** Capric-myristic Acid/Expanded Perlite Composite as Form-stable Phase Change Material for Latent Heat Thermal Energy Storage *Renewable Energy* 33 2008: pp. 2599–605.  
<https://doi.org/10.1016/j.renene.2008.02.024>
27. **Fang, G.Y., Li, H., Chen, Z., Liu, X.** Preparation and Characterization of Stearic Acid/Expanded Graphite Composites as Thermal Energy Storage Materials *Energy* 35 2010: pp. 4622–4626.  
<https://doi.org/10.1016/j.energy.2010.09.046>
28. **Xu, B.W., Li, Z.J.** Paraffin/Diatomite Composite Phase Change Material Incorporated Cement-based Composite for Thermal Energy Storage *Applied Energy* 105 2013: pp. 229–237.  
<https://doi.org/10.1016/j.apenergy.2013.01.005>
29. **Aydin, A.A., Okutan, H.** Polyurethane Rigid Foam Composites Incorporated with Fatty Acid Ester-based Phase Change Material *Energy Conversion & Management* 68 2013: pp. 74–81.  
<https://doi.org/10.1016/j.enconman.2012.12.015>
30. **Sari, A., Sari, H., Onal, A.** Thermal Properties and Thermal Reliability of Eutectics Mixtures of Some Fatty Acids as Latent Heat Storage Materials *Energy Conversion & Management* 45 2004: pp. 365–376.  
[https://doi.org/10.1016/S0196-8904\(03\)00154-7](https://doi.org/10.1016/S0196-8904(03)00154-7)
31. **Sari, A.** Eutectics Mixtures of Some Fatty Acids for Latent Heat Storage: Thermal Properties and Thermal Reliability with Respect to Thermal Cycling *Energy Conversion & Management* 47 2006: pp. 1207–1221.  
<https://doi.org/10.1016/j.enconman.2005.07.005>
32. **Cao, L., Tang, Y.J., Fang, G.Y.** Preparation and Properties of Shape-stabilized Phase Change Materials Based on Fatty acid Eutectics and Cellulose Composites for Thermal Energy Storage *Energy* 80 2015: pp. 98–103.  
<http://doi.org/10.1016/j.energy.2014.11.046>
33. **Tang, F., Su, D., Tang, Y.J., Fang, G.Y.** Preparation and Thermal Properties of Fatty Acid Eutectics and Diatomite Composites as Shape-stabilized Phase Change Materials with Enhanced Thermal Conductivity *Solar Energy Materials & Solar Cells* 141 2015: pp. 218–224.  
<http://doi.org/10.1016/j.solmat.2015.05.045>
34. **Zhang, Y.P., Su, Y.H., Ge, X.S.** Prediction of the Melting Temperature and the Fusion Heat of (Quasi-)Eutectics PCM *Journal of China University of Science and Technology* 25 (4) 1995: pp. 474–478.
35. **He, Y., Zhang, X., Zhang, Y.J., Song, Q., Liao, X.M.** Utilization of Lauric Acid-Myristic Acid/Expanded Graphite Phase Change Materials to Improve Thermal Properties of Cement Mortar *Energy and Buildings* 133 2016: pp. 547–558.  
<http://doi.org/10.1016/j.enbuild.2016.10.016>
36. **Qu, M.J., Guo, C.G., Li, L.P., Zhang, X.C.** Preparation and Investigation on Tetradecanol and Myristic Acid/Cellulose Form-stable Phase Change Material *Journal of Thermal Analysis and Calorimetry* 130 (2) 2017: pp. 781–790.  
<http://doi.org/10.1007/s10973-017-6440-z>
37. **Tang, Y.J., Guruprasad, A., Huang, X., Su, D., Liu, L.K., Fang, G.Y.** Thermal Properties and Morphologies of MA–SA Eutectics/CNTs as Composite PCMs in Thermal Energy Storage *Energy and Buildings* 127 2016: pp. 603–610.  
<http://doi.org/10.1016/j.enbuild.2016.06.031>
38. **Wu, X.J., Li, J.Y., Ma, F.** Preparation and Properties of Hexadecanol-stearic Acid/Bamboo Charcoal Composite *Energy Sources, Part A: Recovery, Utilization, and Environmental Effects* 40(9) 2018: pp. 1044–1050.  
<https://doi.org/10.1080/15567036.2018.1468515>

